Geotech Geol Eng (2022) 40:1887–1898
https://doi.org/10.1007/s10706-021-01998-3

ORIGINAL PAPER

Geotechnical Properties Determination of Thickened Fluid Fine Tailings

Alebachew Demoz

Received: 15 January 2021 / Accepted: 30 September 2021 / Published online: 22 February 2022

Abstract Fluid fine tailings (FFT) comprising clayey-silt solids pose environmental and financial challenges. Currently, mining operators are depositing thickened FFT in deep-pits counting on self-weight consolidation to form stable ground. The motivation of this study is to model the long-term prospects of such deposits utilizing consolidation and direct shear strength measurements. The tests were conducted using scroll decanter centrifuge separated FFT sediment referred to as cake. Drained direct shear tests of the cake gave a linear Mohr–Coulomb failure envelope of 1.2 kPa cohesion intercept and 9° internal friction angle for normal stresses up to 1 MPa. Hydraulic conductivity of the cake was non-linear with normal stress decreasing to 1.7×10^{-11} m/s at 300 kPa. Consolidation results confirmed that the cake exhibits properties similar to those of active clay minerals. The cake compression index is governed by the same relationship as for active clays. The coefficient of consolidation for the cake was nearly constant and had a mean value of 2.25×10^{-3} m^2/y, also similar to that of active clays. The void ratio—effective stress—hydraulic conductivity power law empirical relations were used to simulate settlement with a finite-strain model. Numerical results show that the top portion of an FFT deep-pit deposit remains in the liquid state while the lower portion whose maximum solids content converges to 74% is in plastic state. These mean that options that improve hydraulic conductivity and increase the shear strength of the thickened FFT should be integrated prior to final placement in order to create stable ground.

Keywords Fluid fine tailings · Thickened tailings · Oil sand tailings · Consolidation · Mohr–Coulomb failure envelope · Hydraulic conductivity

1 Introduction

In the extraction of minerals water is used in grinding, transporting, conditioning, cleaning, and separation of the valuable mineral from gangue. The process generates large amounts of mine waste tailings in the form of slurry. Considering the hot-water extraction of bitumen from surface-mined oil sands specifically, a 10% (mass basis) oil-containing ore generates a 55% solids discharge which is 82% sand and 17% fines (Chalaturnyk et al. 2002). Upon discharge, the entire coarse solids with some fraction of trapped fines settles out quickly while the rest of the fines flows into tailings ponds. There is in excess of 1.25 Bm^3 of fluid fine tailings (FFT) in containment ponds from this operation in Northern Alberta (AER 2019) alone. Other mineral resource extractions, such as phosphate

A. Demoz (✉)
Natural Resources Canada, CanmetENERGY, 1 Oil Patch Drive, Devon, AB T9G 1A8, Canada
e-mail: alebachew.demoz@NRCan-RNCan.gc.ca

and bauxite mining, equally produce large volumes of FFT that have similar characteristics as the FFT of oil sands. These FFT are discharged into containment ponds for water recovery and further processing for final disposal. Moreover, the ponds afford long term storage to stagger reclamation activities and time to apply emerging reclamation technologies. The FFT of tailings ponds eventually form a persistent suspension (referred to as mature fine tailings) whose solids mass relative to the wet mass plateaus to under 40% (w/w) in the case of oil sands extraction. These ponds pose major concerns as they require perpetual observation, construction, maintenance, risk of dam failure and increasing long-term liabilities. In response government departments place regulations to ensure safe operation and restoration to dry ground of tailings ponds at end of mine life (AER 2016). Reducing the water content—dewatering (thickening)—is a necessary step for restoration of the FFT ponds as a dry ground. All current commercial technologies for dewatering FFT start with the addition of flocculants and coagulants, which gather the suspended fine particles to form larger and denser aggregates, making them more amenable to subsequent processes.

The industry currently uses a few well-known tailings management methods for final tailings disposal after flocculation. Those methods are thin-lift drying, deep-pit deposition of flocculated FFT (also known as rim-ditch accelerated dewatering), and deposition of thickened tailings after separation using scroll decanter centrifugation (SDC) (BGC 2010). All these technologies in practice result in a thickened FFT whose dry solids content relative to the total wet mass converges to a maximum of about 60 solids% (w/w). At a void ratio of about 1.6, such a deposit of fine solids lacks strength to form a stable ground. In this study we investigated whether or not such a deposit can in the long term become the anticipated reclamation-ready deposit by self-weight consolidation as a vast amount of it is being deposited in thickened form.

The purpose of the research described here was to determine (i) the geotechnical properties of thickened FFT to assess whether thickened FFT can form stable dry ground as a deposit, and (ii) conduct measurements to obtain constants for numerical modelling to predict settlement. Thickened FFT samples obtained using SDC separation, commonly referred to as cake, was used in this study. The cake by conventional categorization can be considered a thickened tailings sample (50–70% w/w). The initial solids content of the sample was 57% (w/w) with liquid and plastic limits of 61% and 16%, respectively and other properties are as given in Table 1. As a specimen the cake is no different from FFT sample that is dewatered to the same void ratio through other routes, such as thickening or consolidation in deep pits. The majority of studies on FFT consolidation were mainly conducted starting with high-void-ratio slurries (Been and Sills 1981; Pollock 1988; Jeeravipoolvarn et al. 2009). For this reason, there is a scarcity of data on the geotechnical properties of FFT with void ratios less than or equal to 2, particularly for oil sands FFT (McKenna et al. 2016; Yao 2016). Therefore, starting with cake sample extends the consolidation study to a stage beyond which this kind of tailings has so far been investigated.

Two types of studies were conducted to determine the geotechnical properties of the cake: consolidation and drained direct shear tests. Consolidation

Table 1 Characteristics of FFT used for this study

Parameter	FFT
Specific gravity of solids (Gs)	2.4
Water content (%)	178
Initial solids (%)	36
Fines content (%)	98
Void ratio	4.27
Clay size (%)[a]	58
Clay size (%)[b]	91
Bitumen content (%)	2.72
Index properties	Cake
Liquid limit (%)	61
Plastic limit (%)	16
Plasticity index (%)	45
Activity	0.77
USCS classification	CH
Grain size (determined by sedigraph)	
D_{10} (μm)[c]	0.30
D_{30} (μm)	0.58
D_{50} (μm)	1.37
D_{60} (μm)	2.18

CH high-plasticity clay; *D* diameter; *FFT* fluid fine tailings; *USCS* Unified Soil Classification System

[a]From methylene blue titration

[b]Particles < 2 (μm in size

[c]Limit of sedigraph measurement

measurements are taken to determine the compressibility and hydraulic conductivity of thickened FFT. Compression and hydraulic conductivity constitutive equations were determined, as they provide constants for model program inputs to predict the rate of settlement of deposits created using thickened FFT. Drained direct shear strength studies of the consolidated thickened FFT (cake) were conducted to determine their Mohr–Coulomb failure envelope. The shear strength of the cake enables estimation of the bearing capacities of thickened tailings (Cernica 1995; Skempton 1964). The two complementary studies provide information about the prospects of creating dry ground out of thickened oil sands FFT deposits. Although the origin of the cake sample is oil sands operations, the results are relevant to other mining tailings whose solids consist predominantly silts and clay fines.

2 Materials and Methods

The FFT used in this study was obtained from one of the major oil sands operators in northern Alberta. Samples were taken from a single batch of 10 m^3 of mature fine tailings (MFT) directly transported from the tailings pond for tailings management program. MFT refers to FFT that has undergone settlement for a few years and is a consistent gel-like sludge that shows no change in physical properties over time. The solids content of the MFT as received was 36% (w/w) (dry solids mass/total mass of sample).

2.1 Particle Size Determination

The special procedure developed for determination of FFT PSD begins with cleaning of the solids using Dean–Stark extraction (Dean and Stark 1920). The extraction removes residual hydrocarbon (bitumen) which interferes with the measurement. The dry clean mineral solids were then disaggregated in a mortar and pestle with care so as not to grind the particles. Prior to measurement the solids were further dispersed in a $NaHCO_3$ buffer at pH 9.6 aided by heating and 20 min of sonication in a bath. PSD were measured with a Sedigraph™ 5100 (MicroMeritics, Norcross, GA, USA). The analysis is based on the settling rate of particles in liquid as measured by the transmittance of a narrow beam of X-ray. Details of the method is found in ISO 13317–3. PSD of the FFT slurry is given in Fig. 1. PSD of the FFT from the oil sands operator from whose tailings pond the sample was obtained is consistent not only within the same batch but even between different batches as can be compared with that reported in Demoz (2015).

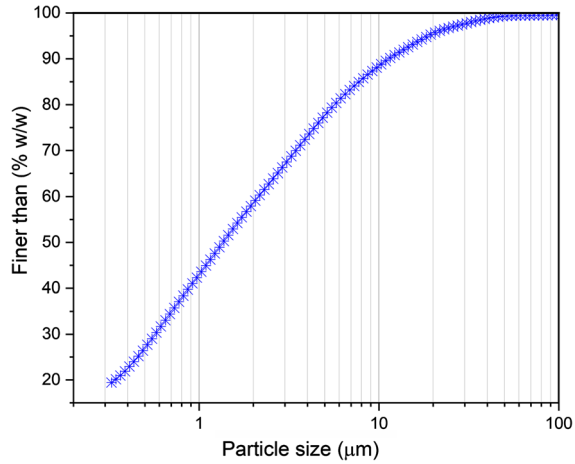

Fig. 1 Particle size distribution of FFT sample obtained using the SediGraph X-ray absorption method

2.2 Methylene Blue (MB) Test

MB spot test for the determination of clay content including those of the American Society for Testing and Materials (ASTM) are based on the cationic MB adsorption and the first stable appearance (5 min) of a blue halo color on filter paper at titration equivalence point (ASTM 1984; Chiappone et al. 2004). To ensure complete interaction of MB with the FFT solids the standard methods were modified with additional cleaning and dispersion to handle oil sands samples (Currie et al. 2014; Young and Sethi 1981).

MB titration of the solids after Dean–Stark extraction gave 12.73 mequiv per 100 g solids, which translates to a calculated clay content of 91 mass%. In contrast, MB titration of the as-received FFT slurry titration gave a clay content of 58 mass% which is more representative of the actual tailings. The difference in clay content between the two methods is known to arise from the effect of sample preparation on surface area.

2.3 Thickened FFT Sample

Thickened samples were prepared by solid–liquid separation of the FFT using SDC. The FFT was first diluted to 23% solids (mass of solids/total sample mass) in a holding tank and flocculated using inline static mixers before the SDC inlet. The SDC was operated so that > 99% of the FFT solids was captured as cake. The cake sample was kept in sealed 20 L pails. The full details of the FFT continuous SDC separation process is found in Demoz (2018).

2.4 Atterberg Limit Measurements

The plastic limit was measured using the soil-thread method in accordance with ASTM Standard D4318-10 (ASTM 2007). The liquid limit, W_L, was measured following the ASTM cone penetration method ASTM D3441-16 (ASTM 2016).

2.5 Direct Shear Strength Measurement

The shear strength of specimens was measured using the direct shear test method ASTM D3080-98 (ASTM 1998). A 100 mm circular shearbox was filled with the saturated pasty cake specimen (57.5% w/w solids) directly using a spatula. The samples solids contents varied by < 0.5% w/w from sample to sample. The pasty cake was easily worked by hand and also using circular aluminum pusher to completely fill the shearbox. Drainage was facilitated by placing the cake between two porous stones: one underneath the stainless steel vertical-force loading pad and the other above the bottom stainless steel retaining grid of the shearbox. To maintain the saturation of the sample, deionized water was added around the edges of the stainless steel loading pad as needed and there was process water in the shearbox carriage all the time. A high-vacuum grease (Dow Corning Corp. Midland, MI, USA) was lightly applied around the edges of the shearbox to reduce edge-to-edge friction and to seal any gaps around the edges of the shearbox.

Drained direct shear test was carried in two phases. The first phase was consolidation under the test normal stress. Multiple smaller load steps had to be used to reach the test normal stress because otherwise the FFT would exude around the edges of the shearbox. The consolidated specimen was thereafter sheared for 10 mm horizontal displacement at a slow rate of 0.025 mm/min while the test normal stress was maintained constant. This shear rate was assessed to be sufficient for excess pore pressure that could develop during shearing to drain. The direct shear test instrument used was a Humboldt E5706 instrument (Humboldt Mfg. Co., Elgin, IL, USA). This equipment is instrumented for automatic logging of vertical and horizontal displacement using linear variable displacement transducers (LVDTs). Both horizontal and vertical loads were measured by 10 kN maximum load cells. Normal load on sample was applied using pneumatic method. A geared stepper motor applied horizontal deformation.

2.6 Compressibility Measurement

The compressibility behaviour of the cake was measured using the Humboldt E5706 instrument, too, but operated as a consolidometer (oedometer). Cake sample preparation and normal stress application for the compression tests were the same as for the direct shear tests. The normal stress was increased sequentially following ASTM D2435-11 (ASTM 2011). Monitoring of the outputs of the Humboldt E5706 LVDTs and control of the instrument were all done by a computer using NEXT^{TM} application software from Humboldt Mfg. Co.

2.7 Hydraulic Conductivity Measurement

Hydraulic conductivity of the cake was measured in a large-strain consolidation (LSC) cell. Small constant heads provided low-pressure gradients for hydraulic conductivity measurements. The particular cell design and its use for permeability measurements are well referenced in many publications of the University of Alberta, Department of Civil and Environmental Engineering (e.g., Suthaker and Scott 1994; Scott et al. 2008). The constant head permeability measurement method was selected because it allows for extremely small head drop tests.

3 Results and discussion

3.1 Direct shear strength

Most reports of the shear strength of flocculated fine tailings are from undrained strengths obtained using

field vane or cone penetration testing (Elias and Beier 2017; Fisseha 2020; Sobkowicz 2013; Wilson et al. 2018). Any drained shear strength measurement via direct shear test of oil sands tailings available in the literature thus far has been on samples that have a sizeable fraction of coarse particles as well, which is not representative of the large inventory of FFT being held in tailings ponds (Fisseha 2020; Kouakou 2014).

Direct shear testing has long been used to estimate drained shear strength parameters of soil for use in the analysis of slope-stability, retaining-wall, and bearing-capacity problems (Cernica 1995; Skempton 1964). In direct shear testing the sample is sheared in a prescribed plane, and although this may be an issue for soils that have developed structure, it is less relevant for uniform, short-lived specimens like FFT cake. The grain sizes of the cake (see Fig. 1) are small, and shear can develop within the cake without any influence from the edges of the shearbox (Palmeira and Milligan 1989).

Drained shear strength of clays and silts depends on factors such as the mineralogical composition of the grains, grain size, grain shape, surface texture, grading, moisture content, normal stress and shear rate. The PSD of the FFT and the Atterberg limits of the cake are shown in Fig. 1 and Table 1, respectively. The PSD shows that the FFT solid particles can be considered 100% fines. The D_{10} value for the cake was below the detection limit of the measurement method used, which is 0.3 µm. The coefficients of curvature and uniformity for the FFT have no relevance as the fines content is way more than 10% (Bowles 1984).

The mean particle size of the FFT is 1.37 µm (Fig. 1). As a clayey material with substantive affinity for water, the long times needed for full consolidation were maintained before the shear strengths were measured. By contrast, just a brief consolidation time is adequate for clean coarse sand, which drains readily, as noted by Kovacs (1997). A soil whose volume remains constant under a constant state of stress can be said to be fully consolidated. When the displacement stops to change, it indicates that the applied stress is born by the grains in the sample and the pore pressure has fully dissipated. For saturated soil the volume change is due to water escape from the voids. In the absence of pore pressure measurement options, the cessation of vertical displacement of specimens was used as the condition of full consolidation in this study. Total pore pressure dissipation is virtually reached when the specimen height ceases to show any change with time. All specimens were consolidated for comparable time periods as that presented in Fig. 4 before starting the direct shear measurements.

The realistic and sustained state of thickened FFT discharge sites is that the deposits remain saturated and open to draining. The direct shear tests were therefore conducted on saturated and drained specimens so as to correspond to real conditions. Figure 2a presents drained direct shear stress versus horizontal displacement at different normal stresses up to that higher than the self-weight of a deep-pit deposit can exert. The shear stress–displacement plot does not display peaks with six of the eight test normal stresses and the shear stress increased with shear displacement without approaching a constant. This is to be expected as peak stress and dilatancy tend to be observed with overconsolidated or dense sandy samples both of which a cake is not. Figure 2b illustrates vertical contraction with horizontal displacement of cake. There were slight contractions which ranged from 1.8% to 4.4% relative to horizontal displacement. In

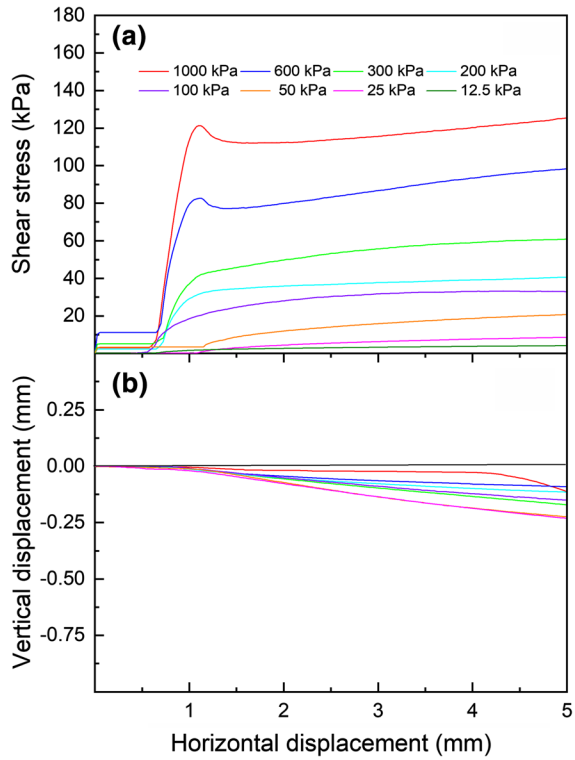

Fig. 2 Curves of shear strength (**a**) and vertical displacement (**b**) versus horizontal displacement for cake in a direct shear test

these kinds of large displacement tests up to 2% of contraction are artifacts of measurements as reported by Bareither et al. (2008). The very small contractions of the cake indicate that the shear zone remained localized in the plane near or at the interface between the two shearbox halves.

Shear failure is frequently associated with the point in the test where the maximum shear stress is reached. The drained direct shear test results show that a shear displacement of 1.2 mm was sufficient to mobilize the peak shear stress; beyond that point the shear stress kept the same plateauing trend. There was also a lag of about 0.5 mm at the start between shear displacement and shear stress. The lag was not specific to the specimen but was equally observed in tests conducted without sample done to determine the shearbox edge-to-edge friction indicating that the lag was due the presence of lateral slack in the shearbox carriage system. Where there is no clearly defined failure point, a select strain can be used as the failure point. In this study the shear stress at 3 mm displacement is reported as the failure shear stress. The uncertainty in shear strength due to this interpretation is minimal because the increase of the measured shear stress with displacement is small. Failure in a soil occurs when the stresses on any plane are such that

$$\tau' = c' + \sigma' tan\phi' \quad (1)$$

where τ' is the effective shear stress at failure; c' is the effective (drained) cohesion intercept; ϕ' is the effective internal friction angle; and σ' is the effective normal stress at failure. The line plotted for shear stress dependence on effective stress forms the Mohr–Coulomb failure envelope, as shown in Fig. 3. The low effective stress plot intercept is very close to the shear strength of fresh cake that is commonly observed using vane shear tools (Sobkowicz 2013).

Some portion of the shear strength is expected to be generated by the friction between the specimen and the edges of the shearbox. To correct for this, shear tests were conducted without any sample but with a thin film of the high-vacuum grease and cake mix applied on the edges of the shearbox. A linear dependence of shear stress and normal stress was observed for the edge effect, and this correlation was used to correct the edge friction effect. The experimental drained shear strength of the cake after correction of the edge friction effect is as presented in Fig. 3.

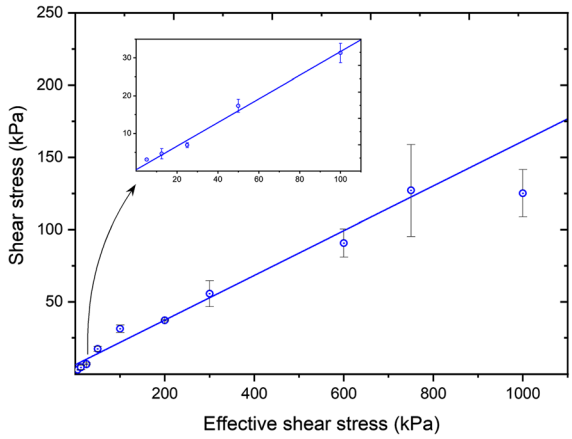

Fig. 3 Shear stress obtained at 3 mm horizontal displacement. Inset shows low confinement stress versus shear stress for a bilinear fit. The error bars are standard deviations from measurements of up to three freshly prepared samples

Generally, the shear strength of freshly produced cakes is around 1.2 kPa at most (Sobkowicz 2013). A constraint of a 1.2 kPa intercept was therefore introduced in deriving the Mohr–Coulomb envelope (Merrien-Soukatchoff and Omraci 2004). The generalized Mohr–Coulomb failure model after correcting for the edge-to-edge friction effect over the test stress range yielded an internal friction angle of 9°. The Mohr–Coulomb failure envelope for the consolidated, drained cake (thickened FFT) tested in this study followed the empirical relationship given below:

$$\tau' = 1.2 + \sigma' tan9 \quad (2)$$

The intercept, τ' and σ' of Eq. 2 are all in kPa. Both the effective cohesion strength and the effective internal friction angle of cake are small. It has been known that the failure envelope at low confinements can differ from that obtained over relatively large confinements (Nafisi et al. 2020). Even nonlinear failure envelopes have been proposed to fit data that could not be expressed with linear failure envelope expressions (Sharma et al. 2011). A bilinear failure envelope can be observed when the confinement stress is limited to two ranges; one for the low confinement range up to100 kPa and an upper confinement range from 200 kPa. A higher internal friction angle of 17° was obtained in the lower confinement range as shown in Fig. 3 inset. The bilinear low confinement fit is relevant for comparison of low confinement stress

measurements but not for practical considerations as high confinements would be required for stable ground formation.

From MB titration and PSD, we determined that the cake is largely made of clay minerals and silt. Its lack of intercalating and cementing minerals explains the small cohesive shear strength of cakes. The cake can be considered a remoulded sample, where no extended structures exist between the fine particles. The strength of a remoulded soil sample is lower than that of a soil in the undisturbed state. The more finer grained particles there are in a soil, the smaller the inclination of the failure envelope, as is also confirmed in this study (Mitchell and Soga 2005). Hu et al. (2017) have reported the strength indices of iron and copper fine tailings whose $D_{50\%}$ were 30 and 60 μm, respectively. The strength indices of both the iron and copper fine tailings were more than three times that of the oil sands fine indices and all three in reverse order with respect to their particle sizes.

The FFT index properties show that the solids have high activity and that their plasticity index (PI) is very high (PI > 40) (Das 1998; Rankka et al. 2004). The index properties indicate that the FFT are composed largely of swelling clay particles. Higher clay contents in a soil cause higher plasticity, greater shrinkage and swell potential, lower hydraulic conductivity, higher compressibility, and lower internal angle of friction, as were observed for the cake. Each of these properties is a drawback for the creation of a stable ground from FFT (Mitchell and Soga 2005).

The deposit needs to be firm to stiff in consistency (i.e., at least 50 kPa shear strength) for it to support small earth-working equipment (McKenna et al. 2016). An effective normal stress of 308 kPa is needed to get a 50 kPa drained shear strength according to Eq. (2). Including the difficulty of laying overburden on high void ratio deposit, the high normal stress threshold indicates that the upper part of a thickened FFT deposit does not have the strength to support earth-working equipment.

3.2 Cake compressibility

The shear strength laboratory analysis above does not give an understanding of the period to attain full consolidation. The vertical deformation of the cake sample from the consolidometer tests is presented in Fig. 4. The time to reach full consolidation is shorter

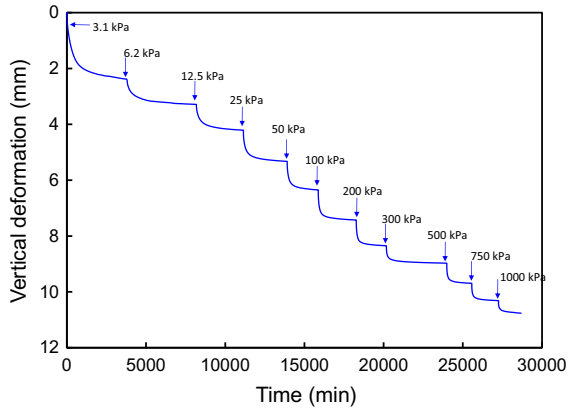

Fig. 4 Vertical deformation versus time data from consolidometer of thickened FFT

the higher the applied normal stress. For instance, the normalized vertical displacement changes after 500 min of consolidation were 60, 89, and 91% of their final settlement at normal stresses of 6.25, 100, and 750 kPa, respectively in this test. The consolidation times at the three stresses in increasing order, for instance, were 73, 41, and 32 h, respectively. Therefore, the consolidation periods were longer at lower loads so as to ensure completeness of primary consolidation.

The void ratio, e–log σ' relationship for ultra-soft soil is nonlinear with a large compression index and no gain in strength (Jeeravipoolvarn et al. 2009). The e–log σ' relationship for the cake was linear, similar to that for soils that naturally have a far smaller compressibility by comparison. The compression index, C_c, of the cake for void ratio from 1.6 to 0.57 was constant and equal to 0.45. This is practically the same as that from the well-known C_c relationship to liquid limit, $C_c = 0.009*(W_L - 10)$, for normally consolidated clays, which for the cake yields $C_c = 0.46$ (Das 1998; Terzaghi et al 1996). The cake C_c is in the middle of the range for silty clays, which is 0.36–0.54, and double that of sandy clays (Whitlow 2001).

A compressibility curve in general may consist of three distinctive regions (Terzaghi et al. 1996; Mitchell and Soga 2005; Khan and Azam 2016). It may start with a horizontal initial portion that pertains to apparent pre-consolidation compression, followed by a linear portion for primary consolidation, and finally by a flatter curve corresponding to secondary compression that is associated with creep settlement.

The cake compression curve exhibited neither the initial horizontal portion nor the post primary compression curve in the studied effective stress range. The absence of an initial flat curve is to be expected, as this was a freshly produced material with no consolidation history. In general, fine tails are underconsolidated and therefore should follow a virgin compression line (Suthaker and Scott 1994). The secondary compression, stage was not observed at the highest applied axial loads, either.

Figure 4 illustrates the settlement of the cake with time at increasing normal loads. In order to express its compressibility, the void ratio at the end of each consolidation stage was calculated using Eq. 3. The vertical displacement data and the void ratio obtained from moisture content measurement after the sample was removed from the consolidometer were used to determine the void ratio and the corresponding effective stress dependence as shown in Fig. 5.

$$\Delta e = \frac{\Delta H}{H_o}(1 + e_o) \tag{3}$$

where e_o is the void ratio and H_o is the corresponding sample height, Δe and ΔH represent changes of these parameters at completion of each consolidation step. The void ratio calculated using Eq. 3 dependence with effective stress is shown in Fig. 5. The best fit curve is also included as part of finding the constitutive equation for effective stress— void ratio relationship. This equation is used to calculate the settlement of cake using the finite strain consolidation model later on. The relationship between void ratio and stress for highly compressible material and soils is often expressed by a power function (Carrier et al. 1983; Pollock 1988). The e–σ' power fit relation below has a best least squares fit correlation factor of 0.98.

$$e = 9.09\sigma'^{-0.197} \tag{4}$$

where σ' is effective stress in Pa.

3.3 Coefficient of consolidation and hydraulic conductivity

The coefficient of volume compressibility, m_v, and the coefficient of consolidation, C_v, dependence on e and σ' are plotted in Fig. 6. C_v is regularly obtained using Terzaghi's infinitesimal-strain consolidation theory (Das 1998; Whitlow 2001). The theory is inapplicable for thickened FFT (cake) because three of the conditions of the infinitesimal theory: specifically very small settlement, linear compressibility and liner permeability were all not observed with this sample.

$$m_v = \frac{\Delta e}{\Delta \sigma'}\left(\frac{1}{1 + e_o}\right) \tag{5}$$

There are other methods besides Terzaghi's consolidation-theory for determining C_v (Islam et al 2020). In this study C_v were determined using Eq. 6. This approach was preferred because it fully relies on the measured parameters of the sample itself.

$$C_v = \frac{k_c}{\gamma_w}\left(\frac{1 + e}{a_v}\right) \tag{6}$$

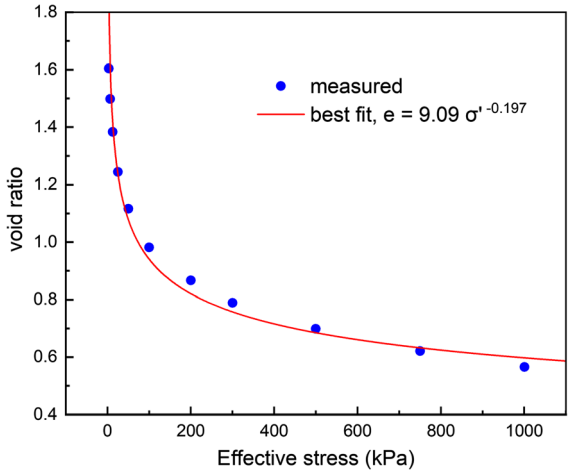

Fig. 5 Power law fit of the volume compressibility curve for cake

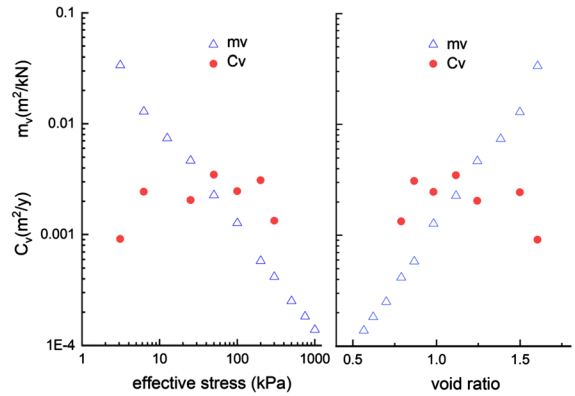

Fig. 6 Coefficients of consolidation and volume compressibility dependence on effective stress and void ratio

where the coefficient of compressibility, a_v, = de/dσ'; k_c is the hydraulic conductivity constant (m/s); and γ_w is the unit weight of water (9.81 kN/m^3). All parameters for eq. [6] were obtained empirically from consolidometer and LSC test results. Cake hydraulic conductivities were measured at a fewer number of effective stresses and up to a maximum effective stress of 300 kPa. In order to increase the reliability of C_v and m_v of Fig. 6 only empirically obtained values were utilized in their calculations.

The mean of the cake C_v is $2.2 \times 10^{-3} \pm 8.5 \times 10^{-4}$ m^2/y, which is in the range reported for active clays (Lambe and Whitman 1979; Mitchell and Soga 2005). As a comparison, C_v of iron, copper and coal fine tailings all are more than two orders of magnitude higher (Hu et al 2017; Islam et al 2020). The value for m_v decreased with increasing σ' and increased with increasing e, as expected. For cake, as for tails with higher water content, an increase in effective stress causes the hydraulic conductivity to decrease due to a significant decrease in void ratio (Pollock 1988; Khan and Azam 2016). The value of m_v varied from 0.03 to 0.0002 m^2/kN, similar to the range measured for underwater dredged fine slurries (Imai et al. 1984).

The cake hydraulic conductivity, k_c, was measured under load using the constant head method (Suthaker and Scott 1994; Scott et al. 2008). Figure 7 shows the k_c of cake at different void ratios. Values of k_c between 10^{-7} m/s^{-1} and 10^{-9} m/s are understood to be poor, whereas deposits with values below that are considered practically impervious (Terzaghi et al. 1996).

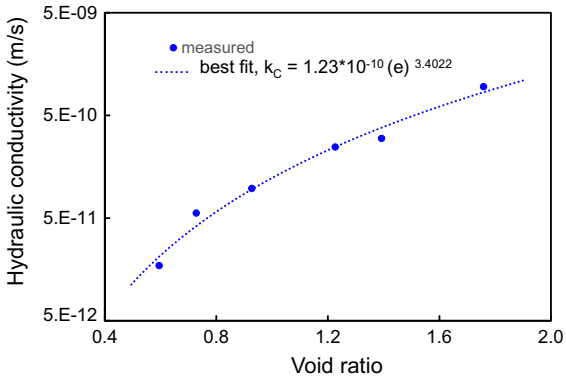

Fig. 7 Saturated hydraulic conductivity dependence on void ratio for cake

The hydraulic conductivity of cake decreased by a factor of about 60 for a decrease in void ratio of only 1. The $k_c - e$ relationship for the cake has the typical power function:

$$k_C = A(e)^B \tag{7}$$

where A is a constant with units of velocity (m/s) and B is dimensionless constant. The values of A and B for the cake are $1.23*10^{-10}$ m/s and 3.40, respectively. These are of similar magnitude to thickened FFT reported by Owolagba and Azzam (2015) as well as for phosphatic clays (Abu-Hejleh et al. 1996; Khan and Azam 2016). Finally having determined the constitutive relations between e and k_c and e and σ' of the cake finite-strain consolidation theory was applied to simulate the settlement of its deposit over long times.

3.4 1D modelling

The question that this study examines is evaluate whether thickened FFT and cake could form timely geotechnically stable deposits. FSConsol, a finite-strain consolidation modelling software (GWP Geo Software Inc., Edmonton, AB) that is widely used in industry, was used for the analyses in this study (Tito 2015). The modelling software is based on the finite-strain settlement solutions given by Gibson et al. (1967, 1981). The application provides the sought outputs of solids content profile with depth and the deep-pit deposit settlement as a function of time (Tito 2015). In addition to the constitutive equations (Eqs. 4 and 7), the inputs of the program include the initial solids content, pit capacity, and rate of filling. To complete the inputs to the model, a 30 m deep pit is set to fill with cake in 8 years and specified to consolidate in two ways; by upward drainage only and drainage through both upward and downward flows. The deposit filling conditions and the constitutive relations used in the simulation are given in Table 2. The fill values are operational subjective choices while the constitutive relations in the right column of the table are fundamental properties of the thickened tailings.

The settlements calculated using the finite-strain consolidation model at 25, 50, 100 and 200 years after the end of filling are 0.39, 0.78, 1.57 and 3.13 m, for upward water drainage only and 0.95, 1.61, 2.68 and

Table 2 Deposit fill conditions and constitutive relations of thickened tailings used in the 1D finite-strain consolidation modelling

Containment type	Pond	Constitutive constants	
Filling condition	Continuous	***Compressibility***	
Filling rate (kg/day)	$13.5*10^6$	coefficient (Pa)	9.09
Containment area (Sq. km)	1.5	exponent	−0.197
Fill height (m)	30	***Hydraulic conductivity***	
Solids Gs	2.4	coefficient (m/s)	$1.23*10^{-10}$
Deposit solids content %(w/w)	57.5	exponent	3.40

4.48 m for double flow conditions, respectively. Figure 8 presents the solid content profile at the same four periods cited above. The increase in solids content begins from the bottom, which is to be expected as it experiences the higher compression. The modelling also shows that the dewatering converges towards a maximum solids content of 74%. The model results show that even after hundreds of years of consolidation the top third of the deposit is in the liquid state, absent the impact of environmental effects such as freeze–thaw and desiccation. As well, the portion of the deposit that consolidates to the maximum solids content is in the plastic state closer to the liquid state as its liquidity index of 0.42 indicates. Realistically, the self-weight consolidated cake or thickened (dewatered) FFT deposit will remain saturated and of such a high moisture content that it cannot by itself be relied on as a route toward reclamation in the form of a dry ground. Similarly, thickening of FFT

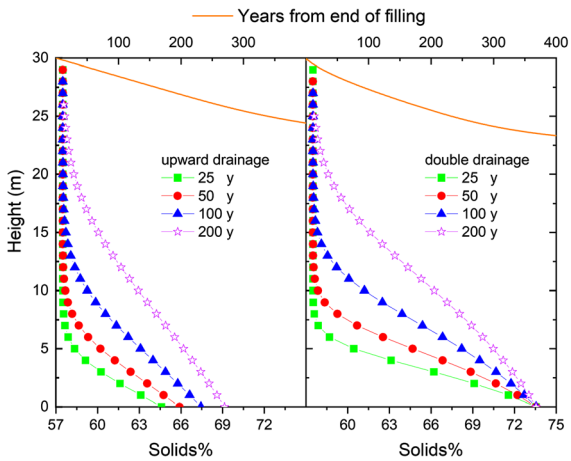

Fig. 8 Finite-strain model calculations showing solid content variation with height of a 30 m cake deposit under upward drainage only or double drainage at the indicated years after completion of filling. The settlement (height change) with time is associated with the secondary abscissa

using filtration gives a deposit no different in properties than that of SDC separation. Backfilling in all its variations is an operation that cannot be exercised with surface mines like the oil sands (Yilmaz et al. 2012). These suggest that co-disposal of the thickened tailings with mine coarse tailings is the only realistic alternative if FFT ponds are to be reclaimed as dryland. The advantages of the co-disposal processing are likely to be realized if the coarse tailings is added into thickened (plastic consistency) FFT rather than the high void ratio slurry (viscous) FFT (Wilson et al. 2018).

4 Summary and conclusion

The large and still increasing inventories of FFT from global mining has serious engineering, environmental and economic costs. The geotechnical properties of FFT from the oil sands extraction were determined to evaluate whether such fine tails can develop into dryland through in-pit consolidation. Direct shear strength for confinement up to 1 MPA gave a linear Mohr–Coulomb failure envelope with very small cohesive intercept and small internal friction angle indicating that even thickened deposits of FFT will remain metastable and liquifiable.

Thickened FFT hydraulic conductivity was very low and similar to that of active clays. The e–σ'–k_c empirical power law curves constitutive constants were used as model inputs to predict tailings settlement using a finite-strain 1D model software. The model output indicated that consolidation by self-weight would take an extremely long time to create reclamation-ready deposits. The implication of this study is that the integration of options in the operation which increase shear strength and hydraulic conductivity are a necessity for stable dryland formation. Co-disposal with available coarse tailings is the realistic

route to improve both the shear strength and hydraulic conductivity. Work is underway to determine analytical relations between hydraulic conductivity and sand-to-fine ratio for co-disposal schemes.

Acknowledgements Funding for this work was provided by the Natural Resources Canada Program of Energy Research and Development. Sincere thanks to colleagues in the Environmental Impacts team, in particular Dr. K. Kasperski for team leadership, and J. Elias and C. McMullen for help with the LSC measurements.

Funding For this work was provided by the Natural Resources Canada Program for Energy Research and Development.

Declarations

Conflict of interest The author has no relevant financial or non-financial interests to disclose.

Code availability FSConsol (GWP Geo Software Inc. Edmonton, AB) is a commercially available software.

Data availability All data used is included in the manuscript and can be provided upon request.

References

Abu-Hejleh AN, Znidarčić D, Barnes BL (1996) Consolidation characteristics of phosphatic clays. J Geotech Eng 122(4):295–301

Alberta Energy Regulator (AER) (2016) Fluid tailings management for oil sands mining projects

Alberta Energy Regulator (AER) (2019) State of fluid tailings management for mineable oil sands, 2018

ASTM (1984) Standard test method for methylene blue index of clay (C 837–99), 1984Annual Book of ASTM Standards, sect. 15, vol. 15.02. American Society for Testing and Materials ASTM, Philadelphia, Pa

ASTM (1998) ASTM D3080–98: Standard test method for direct shear test of soils under consolidated drained conditions. ASTM International, West Conshohocken, PA

ASTM (2007) ASTM D4318–10: Standard test methods for liquid limit, plastic limit, and plasticity index of soils. ASTM International, West Conshohocken, PA

ASTM (2011) ASTM D2435–11: standard test methods for one-dimensional consolidation properties of soils using incremental loading. ASTM International, West Conshohocken, PA

ASTM (2016) ASTM D3441–16: Standard test method for mechanical cone penetration testing of soils. ASTM International, West Conshohocken, PA

Bareither CA, Benson CH, Edil TB (2008) Comparison of shear strength of sand backfills measured in small-scale and large-scale direct shear tests. Can Geotech J 45:1224–1236

Been K, Sills GC (1981) Self-weight consolidation of soft soils. Géotechnique 31:519–535

Beier N, Wilson W, Dunmola A, Sego D (2013) Impact of flocculation-based dewatering on the shear strength of oil sands fine tailings. Can Geotech J 50(9):1001–1007

BGC (2010) Oils sands tailings technology review. OSRIN Report No. TR-1, BGC Engineering Inc., Vancouver, BC. Available from www.infomine.com/library/publications/docs/BGCEngineering2010.pdf [accessed February 2, 2020]

Bowles JE (1984) Physical and geotechnical properties of soils, 2nd edn. McGraw-Hill, New York, NY

Carrier WD, Bromwell LG, Somogyi F (1983) Design capacity of slurried mineral waste ponds. J Geotech Eng Div 109(5):699–716

Cernica JN (1995) Geotechnical engineering soil mechanics. Wiley, Toronto, ON

Chalaturnyk RJ, Scott JD, Ozum B (2002) Management of oil sand tailings. Petrol Sci Technol 20:1025–1046

Chiappone A, Marello S, Scavia C, Setti M (2004) Clay mineral characterization through the methylene blue test: comparison with other experimental techniques and applications of the method. Can Geotech J 41:1168–1178

Currie R, Bansal SI, Khan I, Mian H (2014) An investigation of the methylene blue titration method for clay activity of oil sands samples. https://era.library.ualberta.ca/items/b831aa15-7986-4c6f-a7e8-439f02b1b59d/view/6fb2a0af-dadb-4ee9-acbd-5022ac8d347b/TR-60-20–20MBI-20Report.pdf (accessed on July 28, 2021)

Das BM (1998) Principles of geotechnical engineering, 4th edn. PWS Publishing Company, Boston, MA

Dean EW, Stark DD (1920) A convenient method for the determination of water in petroleum and other organic emulsions. Ind Eng Chem 12(5):486–490

Demoz A (2015) Scaling inline static mixers for flocculation of oil sand mature fine tailings. Am Inst Chem Eng 61(12):4402–4411

Demoz A (2018) Impact of preflocculation on scroll decanter centrifuge separation performance. Can J Chem Eng 96(1):265–269

Devenny DW (2010) A screening study of oil sand tailings technologies and practices. Revision I, March. Alberta Energy Research Institute, prepared for the Government of Alberta. Available from ww@@w.assembly.ab.ca>Iao>library>egovdoc>aleri [accessed February 2 2020]

Elias J, and Beier NA (2017) Effect of floc size on geotechnical properties of oil sands fluid fine tailings: experimental

study. In: Proceedings of the 2017 Tailings & Mine Waste Conference, Banff, AB, 5–8 November 2017. University of Alberta, 733–740

Fisseha BT (2020) Experimental study on consolidation behaviour and shear strength gain for saturated/unsaturated treated fluid fine tailings. PhD thesis. Department of Civil and Environmental Engineering, University of Alberta, Edmonton, AB

Gibson RE, England GL, Hussey MJL (1967) The theory of one-dimensional consolidation of saturated clays. Géotechnique 17(3):261–273

Gibson RE, Schiffman RL, Cargill KW (1981) The theory of one-dimensional consolidation of saturated clays, II. finite non-linear consolidation of thick homogeneous layers. Can Geotech J 18:280–293

Hu L, Wu H, Zhang L, Zhang P, Wen Q (2017) Geotechnical properties of mine tailings. J Mater Civ Eng 29(2):04016220

Imai G, Yano K, Aoki S (1984) Applicability of hydraulic consolidation test for very soft clayey soils. Soils Found 24(2):29–42

Islam S, Williams DJ, Llano-Serna M, Zhang C (2020) Settling, consolidation and shear strength behaviour of coal tailings slurry. Int J Min Sci Technol 30(6):849–857

ISO (2001) 13317–3:2001, Determination of particle size distribution by gravitational liquid sedimentation methods—Part 3: X-ray gravitational technique

Jeeravipoolvarn S, Scott JD, Chalaturnyk RJ (2009) 10 m standpipe tests on oil sands tailings: long-term experimental results and prediction. Can Geotech J 46(8):875–888

Khan FS, Azam S (2016) Determination of consolidation behaviour of clay slurries. Int J Min Sci Technol 26(2):277–283

Kouakou WA (2014) Geotechnical characterization of oil sand tailings beach deposition in flume tests. M.Sc. thesis, Department of Civil and Environmental Engineering, University of Alberta, Edmonton, AB

Kovacs WD (1997) The Karol–Warner direct shear testing machine. Internal Report, University of Washington, Seattle, WA

Lambe TW, Whitman RV (1979) Soil mechanics. Wiley, New York, NY

McKenna G, Mooder B, Burton B, and Jamieson A (2016) Shear strength and density of oil sands fine tailings for reclamation to boreal forest landscape. In: 5th IOSTC International Oil Sands Tailings Conference, Lake Louise, AB, 4–7 December 2016. University of Alberta Geotechnical Group, Edmonton, AB

Merrien-Soukatchoff V, Omraci K (2004) Various assessments of the characteristic values of soil cohesion and friction angle: application to New Caledonian laterite. In: Hack R, Azzam R, Charlier R (eds) Engineering geology for infrastructure planning in Europe: a European perspective. Springer, New York, NY, pp 144–152

Mitchell JK, Soga K (2005) Fundamentals of soil behavior, 3rd edn. Wiley, New York, NY

Nafisi A, Montoya BM, Evans TM (2020) Shear strength envelopes of biocemented sands with varying particle size cementation level. J Geotech Geoenviron Eng. https://doi.org/10.1061/(ASCE)GT.1943-5606.0002201

Owolagba J, Azam S (2015) Geotechnical properties of centrifuged oil sand fine tailings. Environ Geotech 2(5):309–316

Palmeira EM, and Milligan GW (1989) Scale effects in direct shear tests on sand. In: Proceedings of the 12th international conference on soil mechanics and foundation engineering, Rio de Janeiro, Brazil, 13–18 August 1989. Balkema, Rotterdam, Netherlands. pp. 739–742

Pollock GW (1988) Large strain consolidation of oil sands tailings sludge. M.Sc. thesis, Department of Civil Engineering, University of Alberta, Edmonton, AB

Rankka K, Andersson-Skőld Y, Hultén C, Larsson R, Leroux V, and Dahlin T (2004) Quick clay in Sweden. Report No. 65, Swedish Geotechnical Institute, Linkőping, Sweden.

Sharma MSR, Baxter CDP, Hoffmann W, Moran K, Vaziri H (2011) Characterization of weakly cemented sands using nonlinear failure envelopes. Int J Rock Mech Min Sci 1(48):146–151

Scott JD, Jeeravipoolvarn S, Chalaturnyk RJ (2008) Tests for wide range of compressibility and hydraulic conductivity of flocculated tailings. In: Proceedings of the 61st Canadian Geotechnical Conference, Edmonton, AB, 22–24 September. pp. 738–745

Skempton AW (1964) Long term stability of clay slopes. Geotechnique 14:77–107

Sobkowicz JC (2013) Developments in treating and dewatering oil sand tailings. In: R Jewell, AB Fourie, J Caldwell & J Pimenta (eds), Proceedings of the 16th International Seminar on Paste and Thickened Tailings, Australian Centre for Geomechanics, Perth, pp. 3- 18

Suthaker NN, and Scott JD (1994) Consolidation behavior of oil sand fine tailings. In: Proceedings of the American Society for surface mining and reclamation national meeting, Pittsburgh, PA, 24–29 April 1994. Vol. 4, pp. 399–406

Taylor DW (1948) Fundamentals of soil mechanics. Wiley, New York, NY

Terzaghi K, Peak RB, Mesri G (1996) Soil mechanics in engineering practice. John Wiley, New York, NY

Tito AA (2015) Numerical evaluation of one-dimensional large-strain consolidation of mine tailings. M.Sc. thesis, Department of Civil and Environmental Engineering, Colorado State University, Fort Collins, CO

Whitlow R (2001) Basic soil mechanics, 4th edn. Prentice-Hall, Dorchester, UK

Wilson GW, Kabwe LK, Beier NA, Scott JD (2018) Effect of various treatments on consolidation of oil sands fluid fine tailings. Can Geotech J 55(8):1059–1066

Yao Y (2016) Dewatering behaviour of fine oil sand tailings: an experimental study. Ph.D. thesis, Department of Civil Engineering and Geosciences, Delft University of Technology, Delft, Netherlands

Yilmaz E, Belem T, Benzaazoua M (2012) One-dimensional consolidation parameters of cemented paste backfills. Min Resour Manag 28(4):29–45

Yong RN. and Sethi A (1981) Method for determining clay content in tailings and sludge, Canadian Patent# 44529000